Sains Malaysiana 51(4)(2022): 1131-1142
http://doi.org/10.17576/jsm-2022-5104-15

The Senescence Effect of Zoledronate on Three-Dimensional Oral Mucosa Model

(Kesan Senesens Zoledronat pada Model Mukosa Oral Tiga Dimensi)

Nur Bashira Shaharuddin[1], Danial Jones[2] & Wen Lin Chai[1,*]

[1]*Department of Restorative Dentistry, Faculty of Dentistry, University of Malaya, 50603 Kuala Lumpur, Federal Territory, Malaysia*
[2]*Division of Natural Sciences, Indiana Wesleyan University, 4201 S. Washington St., Marion, Indiana, 46953, USA*

Received: 18 October 2020/Accepted: 1 September 2021

ABSTRACT

Zoledronate (ZOL) is an antiresorptive bisphosphonate used to prevent bone loss in skeletal-related disorders, especially in patients with advanced cancer metastatic to bone. However, this medication led to an oral lesion known as medication-related osteonecrosis of the jaw (MRONJ) which also presents clinically as unhealing soft tissue in the jaw. Keratinocytes are thought to be a significant onset factor for MRONJ and recent findings have shown evidence of senescence in keratinocytes. However, little is known about the effect of senescence-associated inflammation that may cause age-associated tissue degeneration, which relates mainly to the expression of extracellular modulators including cytokines known as senescence-associated secretory phenotype (SASP). The aim of this experiment was to investigate the effect of ZOL treatment and senescence-associated secretory phenotype (SASP) if any, on a three-dimensional oral mucosa model (OMM) in which a novel modification was made to reflect the existence of basement membrane (BM) and lamina propria accurately. The ZOL dosage for the model was optimized by exposing the immortalized human oral keratinocyte line (OKF 6/TERT-2) and normal human oral fibroblasts (NHOF) to ZOL at increasing dosages and then histoarchitecture of OMM was examined. Analysis of the model's histology showed significant epithelial thinning upon ZOL treatment and breakage of the BM accompanied by downward proliferation towards the lamina propria. A significant release of SASP molecules (MMP-3 and IL-8) was also detected upon treatment. Therefore, this study suggests that ZOL may impair healing at multiple types of tissues, originally from keratinocytes, by the deleterious effects of the senescence-associated inflammatory response.

Keywords: Oral mucosa; osteonecrosis; senescence; tissue engineering; zoledronate

ABSTRAK

Zoledronat (ZOL) adalah ubat bifosfonat antiresorptif yang digunakan untuk mencegah kehilangan tulang pada gangguan yang berkaitan dengan rangka, terutama pada pesakit yang mengalami barah tulang. Walau bagaimanapun, ubat ini sering menyebabkan lesi pada mulut yang dikenali sebagai osteonekrosis rahang (MRONJ) yang juga dikenali secara klinikal sebagai tisu lembut di rahang yang tidak dapat disembuhkan. Keratinosit dianggap sebagai faktor permulaan yang signifikan untuk MRONJ dan penemuan baru-baru ini telah menunjukkan bukti penuaan pada keratinosit. Walau bagaimanapun, kesan keradangan yang berkaitan dengan kemerosotan tisu berkaitan dengan usia, terutamanya pelahiran modulator ekstrasel termasuk sitokin dikenali sebagai fenotip sekretori yang berkaitan dengan penuaan (SASP). Tujuan penyelidikan ini adalah untuk mengkaji kesan rawatan ZOL dan fenotip sekretori yang berkaitan dengan penuaan (SASP) jika ada, pada model mukosa oral tiga dimensi (OMM) dengan pengubahsuaian baru dibuat untuk mencerminkan adanya membran dasar (BM) dan lamina propria dengan tepat. Dos ZOL untuk model itu dioptimumkan dengan mendedahkan keratinosit oral manusia abadi (OKF 6/TERT-2) dan fibroblas oral manusia normal (NHOF) kepada ZOL pada peningkatan dos dan kemudian struktur tisu OMM diperiksa. Analisis histologi model menunjukkan penipisan epitelium yang signifikan pada rawatan ZOL dan kerosakan BM disertai dengan pertumbuhan keratinosit ke arah lamina propria. Pelepasan molekul SASP yang signifikan (MMP-3 dan IL-8) juga dikesan semasa rawatan. Oleh itu, kajian ini menunjukkan bahawa ZOL kemungkinan besar boleh mengganggu penyembuhan pelbagai jenis tisu, yang bermula dari keratinosit melalui tindak balas keradangan yang berkaitan dengan penuaan.

Kata kunci: Kejuruteraan tisu; mukosa mulut; osteonekrosis; senesens; zoledronat

Introduction

Bisphosphonates (BP) and denosumab are potent antiresorptive agents that can reduce the risk of bone fractures that develop during bone loss diseases, including osteoporosis, Paget's disease, cancer treatment-induced bone loss (CTIBL), cancer metastasis to bone, and multiple myeloma (Nicolatou-Galitis et al. 2019). Because of the growing number of osteonecrosis of the jaw (ONJ) cases, particularly in the oncogenic population (Filleul & Saussez 2010) that require long-term higher dosage and potency of antiresorptive treatment, medication-related osteonecrosis of the jaw (MRONJ) has become a significant health problem that impairs quality of life.

MRONJ manifests as exposed necrotic bone in the maxillofacial region, accompanied by soft tissue lesions that last for more than eight weeks. Although non-exposed MRONJ has also been recognized (Reid 2009), more cases demonstrated necrotic bone appearance after the oral mucosa has been compromised due to invasive dental treatment or bacterial infection (Reid 2009). Scientists have demonstrated that bisphosphonate, particularly on nitrogen-containing bisphosphonate (N-BP) including zoledronate induces senescence in oral keratinocytes and leads to impaired migration and proliferation in a wound healing model (Kim et al. 2011). However, despite being dormant in replication activity, senescent cells are metabolically active in secreting factors that affect the tissue microenvironment, a phenomenon known as the senescence-associated secretory phenotype (SASP) (Campisi & d'Adda di Fagagna 2007). The SASP can be beneficial to reinforce senescence growth arrest by an autocrine cytokine network, thereby arresting the growth of cells at risk for neoplastic transformation and initiating tissue repair. However, when chronically present, the tissue may enter a pro-inflammatory state that may be deleterious by disrupting normal tissue structure and function and eventually stimulating age-associated tissue degeneration or promoting malignant phenotypes (Coppe et al. 2010). To date, 3-dimensional *in vitro* models that reflect the complexity of the oral mucosa are limited to construct oral keratinocytes embedded in collagen populated with fibroblasts, which lack intact basement membrane (BM) (Bae et al. 2014; Scheper et al. 2010). To further clarify the effects of senescence on oral mucosa tissues, this study investigated whether the effect of ZOL involved the senescence-associated inflammatory response and whether that effect influenced the integrity of oral mucosa in an updated tissue construct.

Materials and Methods

Cells and cell culture

A small piece of gingival tissue was taken from healthy individuals during wisdom tooth removal. This study has received the Medical Ethics Committee approval (No. DFDP1406/0061(L). Half of the biopsies were formalin-fixed, paraffin-embedded (FFPE) as a control for the oral mucosa model experiments. The connective tissue was separated from the epidermis by overnight incubation in 0.4 mg/mL dispase at 4 °C. Fibroblasts were isolated by incubation in 0.05% (w/v) collagenase type I (Gibco, Thermo Fischer Scientific Company, Waltham, USA) at 37 °C for overnight. After 24 h of incubation, the tissue suspension was centrifuged at 1000 rpm for 5 min. The isolated NHOFs were cultured in complete Dulbecco Modified Eagle Medium (DMEM) (Gibco, Thermo Fisher Scientific Company, Waltham, Massachusetts, United States), which was supplemented with 10% fetal bovine serum, penicillin-streptomycin 100 µg/mL, 100 units/mL, 0.25 µg/mL of amphotericin B and 2 mM Glutamax. OKF 6/TERT-2s were cultured in keratinocyte-SFM media (K-SFM) containing penicillin-streptomycin 100 µg/mL, 100 units/mL in 10 mM citrate buffer and 30 µg/mL bovine pituitary extract (BPE) supplemented with 0.1 ng/mL epidermal growth factor (EGF) (Gibco, Thermo Fisher Scientific Company, Waltham, Massachusetts, United States) and 0.4 mM $CaCl_2$ (Sigma Aldrich, St. Louis, Missouri, United States). Growth kinetics and cell seeding optimization experiments were performed to ensure that cells were in the proliferative phase before drug treatment in monolayer and 3D cultures (data not shown).

Reagents

Zoledronic acid (Sigma Aldrich, St. Louis, Missouri, United States) was dissolved in 0.1 N sodium hydroxide (NaOH). 5-Aza-2'-deoxycytidine (5-Aza-CdR; Enzo, Enzo Life Sciences, Farmingdale, New York, United States) is a specific inhibitor of DNA methylation. 5-Aza-CdR was solubilized in dimethyl sulfoxide (DMSO; Sigma Aldrich, St. Louis, Missouri, United States) to a final concentration in the media of 0.006% and used at 3 µM as a positive control for senescence experiments.

Cell viability assay

NHOFs from passage 3-5 (1×10^3 cells/well) and OKF 6/TERT-2s (2×10^3 cells/well) were plated in 96-well microculture plates. After 48 h in culture, cells were

incubated with ZOL in increasing concentrations of 0 (vehicle only), 1, 3, 10, 30, 100, 300, and 1000 µM for each for 24, 48, and 72 h. Cell viability was measured using MTT colorimetric assays (Roche Diagnostics, Indianapolis, Indiana, United States) according to the manufacturer's instructions. Optical density was measured at 570 nm with a reference wavelength of 690 nm. All experiments were performed in triplicate, while the percent viability was normalized to that of non-treated cells.

IMMUNOFLUORESCENCE

After growth on coverslips, OKF 6/TERT-2 cells were treated with 3 µM 5-Aza-CdR for 120 h. Cells were fixed with 4% fresh paraformaldehyde for 15 min at room temperature. After gentle washing with PBS, cells were then permeabilized using 1% Triton X-100 (Merck KGaA, Darmstadt, Germany) (30 min). Cells were blocked for 1 h at room temperature (RT) in a blocking solution containing 5% bovine serum albumin (BSA; Thermo Scientific, Thermo Fisher Scientific, Waltham, Massachusetts, United States). Both primary and secondary antibodies were purchased from Santa Cruz Biotechnology (Dallas, Texas, United States). The primary antibody, rabbit anti-p15 polyclonal antibody (#sc-28260), was diluted to 1:50 with 1% BSA for overnight incubation at 4 °C. After incubation with a primary antibody, cells were washed in PBS and then incubated with secondary fluorochrome-conjugated antibody (mouse anti-rabbit IgG-FITC, #sc-2359), diluted to 1:75 for 1 h at RT. Both antibodies were validated previously for immunofluorescence detection in human cells (Yuan et al. 2013). To counterstain, Fluoroshield™ with DAPI (Sigma Aldrich, St. Louis, Missouri, United States) was added onto a glass slide, and the coverslip was mounted. The stained sections were visualized with a Leica DMI3000 inverted microscope with fluorescence (Leica Microsystems, Milton Keynes, Bucks, United Kingdom).

STAINING FOR SENESCENCE-ASSOCIATED ß-GALACTOSIDASE (SA B-GAL)

To assess senescence in keratinocytes treated with ZOL, SA β-Gal activity was measured using a senescence detection kit (Biovision Inc., Milpitas, California, United States) according to the manufacturer's instructions. OKF 6/TERT-2s and NHOFs were cultured at 15000 cells/cm^2 and 2400 cells/cm^2, respectively, in 24-well plates. After 48 h in culture, cells were treated with 12 µM ZOL, 3 µM 5-Aza-CdR, or control (vehicle only) for 48 h before the SA β-Gal assay was conducted. After adding the staining solution containing 1 mg/mL 5-Bromo-4-chloro-3-indolyl-β-D-galactosidase, cells were incubated at 37 °C overnight and counterstained with eosin. The positive SA β-Gal activity was determined by the percentage of blue-stained cells over total cells in 10 random microscopic fields under 20X magnification.

FABRICATION OF A THREE-DIMENSIONAL OMM AND ADMINISTRATION OF ZOLEDRONIC ACID

An OMM consisting of a multilayer of OKF 6/TERT-2s grown on the acellular cadaveric dermis, AlloDerm GBR ® (LifeCell Corporation, Branchburg, New Jersey, United States) in which NHOFs were embedded to create a stromal-like structure with an intact BM, was constructed as previously described (Tra et al. 2012). OKF 6/TERT-2s were gently seeded onto the BM surface of the acellular dermis. After 2 h of seeding, the medium was gently replaced with K-SFM media supplemented with 30 µg/mL of bovine pituitary extract, penicillin-streptomycin 100 µg/mL, 100 units/mL, 1 ng/mL epidermal growth factor (EGF), and 0.4 mM $CaCl_2$. The OMM was cultured in a submerged condition for four days with medium changed every 48 h. The OMM was then airlifted for another three days to allow OKF 6/TERT-2s to differentiate and stratify in K-SFM media supplemented with 0.025 mM glucose (Gibco, Thermo Fisher Scientific Company, Waltham, Massachusetts, United States), 1.2 mM $CaCl_2$, and 10% fetal bovine serum. After three days of air-liquid interface culture, the OMM was continuously fed with growth medium only, medium containing 12 µM ZOL, or medium containing 3 µM 5-Aza-CDR for another 48 h. The 3D models were then harvested, formalin-fixed, paraffin-embedded (FFPE), and stained with hematoxylin and eosin (H&E).

IMMUNOHISTOCHEMISTRY

The detection system for the immunohistochemical staining was the Vectastain Universal ELITE ABC kit (Vectastain®, Vector Lab Incorporated, Burlingame, California, United States). Immunohistochemical staining was performed according to the manufacturer›s instructions as previously described (Goodpaster et al. 2008). For the antigen retrieval procedure, tissue sections were incubated with 0.05% trypsin (Gibco, Thermo Fisher Scientific, Waltham, Massachusetts, United States) containing 1% calcium chloride for 20 min at 37 °C. Mouse anti-cytokeratin 10/13 human monoclonal primary antibody (Santa Cruz Biotechnology, Dallas, Texas, United

States, #sc-6258) was used at 1:50, and incubation was performed at 4 °C overnight. Images were taken with a digital slide scanner Pannoramic™ DESK II (3D Histech, Budapest, Hungary).

QUANTIFICATION OF EPITHELIAL THICKNESS

The slides were all photographed and examined using a Pannoramic™ DESK digital slide scanner (3D Histech, Budapest, Hungary) at different magnifications. Using the Pannoramic Scanner software, the epithelial layer's thickness (the linear distance perpendicular to the AlloDerm between the basal surface of basal cells and the keratinized layer) was measured at 13 random points per section. The mean of 13 values was assigned to the thickness of the sample.

DETECTION OF SENESCENCE-RELATED CYTOKINES IN THE SUPERNATANTS

The senescence-associated secretory phenotype (SASP) molecules MMP-3 and IL-8 from oral mucosa models were assessed with enzyme-linked immunosorbent assays (Quantikine® Immunoassay Systems, R&D Systems, Minneapolis, Minnesota, United States) following drug treatment for 48 h. The untreated oral mucosa model served as a control, and experiments were performed in triplicate on three occasions. The optical density value was read on an ELISA multi-plate reader (Thermo Fisher Scientific, Waltham, Massachusetts, United States) with an absorbance wavelength of 450 nm and correction at 570 nm.

STATISTICAL ANALYSIS

Results were expressed as mean ± standard deviation, with n referring to the number of experiments. A non-linear regression analysis was performed to determine the best-fit value of IC_{50}. Differences among exposure times were determined using the extra sum of the squares F test. A p value less than .05 was considered significant. The ANOVA and Tukey's post hoc test were applied to determine the differences among means for senescence-related cytokine expression and epithelial thickness of the oral mucosa model in response to the drug treatment (SPSS v. 12.0.1, SPSS, Chicago, Illinois, United States).

RESULTS

CELL VIABILITY AND IC_{50} DETERMINATIONS IN RESPONSE TO ZOL TREATMENT

To examine the direct effect of ZOL on oral mucosal cells, MTT assays were first performed on cells exposed to various concentrations of ZOL. Interestingly, the IC_{50} value doses for NHOFs were relatively toxic to OKF 6/TERT-2s (Table 1).

TABLE 1. 50% inhibitory concentration (IC_{50}) was reported from MTT viability assays of normal human oral fibroblasts (NHOF) and immortalized oral keratinocytes (OKF 6/TERT-2) treated with ZOL following 24, 48, and 72 h of incubation. Data were reported as mean IC_{50} value ± S.D. from three independent experiments determined from a non-linear regression analysis

Incubation time (h)	IC_{50} NHOF (μM)	IC_{50} OKF6/TERT-2 (μM)
24	349.8 ± 1.1	10.0 ± 1.3
48	49.3 ± 1.4	12.4 ± 1.7
72	15.8 ± 1.1	1.0± 1.3

Therefore, the concentration used in the oral mucosa model was based upon the IC_{50} value in OKF 6/TERT-2s. As a result, treatment of 12 μM ZOL for 48 h was regarded as appropriate to be utilized in 3D culture and corresponded to a 71 and 50% viability for NHOF and OKF 6/TERT-2 monolayer cells, respectively (Figure 1(A) & 1(B)).

IMMUNOFLUORESCENT VISUALIZATION OF THE P15 SENESCENCE MARKER IN ZOL-TREATED OKF 6/TERT-2 CELLS

To date, no study investigates evidence of senescence in immortalized oral keratinocytes (OKF 6/TERT-2 cells). To confirm the potential of OKF 6/TERT-2s to undergo senescence, the expression of p15, a known marker of senescence, was tested against a p15 antibody via indirect immunofluorescence. OKF 6/TERT-2s expressed p15 protein in response to 5-Aza-CdR, while p15 signal was not detected in non-treated cells (Figure 2).

Based on these results, 5-Aza-CdR was used to induce senescence in the oral mucosa model to serve as a control in demonstrating how ZOL induces senescence in the model.

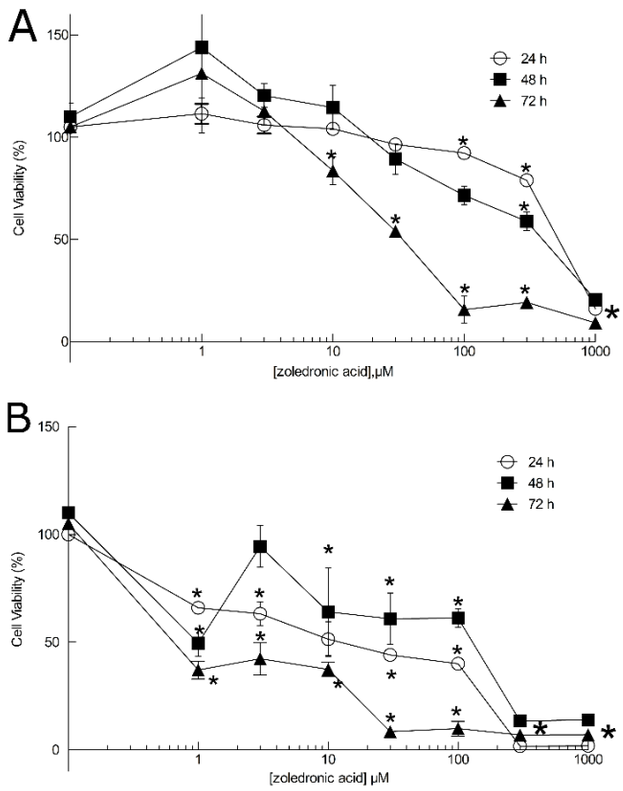

FIGURE 1. Effects of ZOL on A) normal human oral fibroblast cell (NHOF) and B) OKF 6/TERT-2 cell viability at different incubation times of 24, 48, and 72 h. The asterisks (*) represent statistically significant differences compared to untreated cells ($P \leq 0.05$, n = 3)

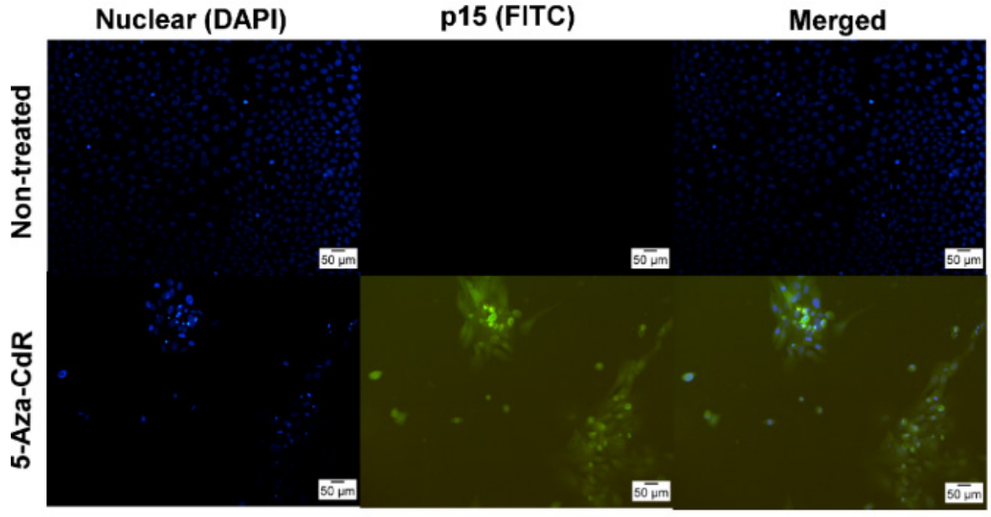

FIGURE 2. Immunofluorescence microscopy images of OKF 6/TERT-2 cells treated with 3 μM 5-Aza-CdR showing that p15, a known senescence marker, was expressed in response to the positive senescence control. Non-treated cells are in the top panel, and 5-Aza-CdR-treated cells are in the bottom panel with nuclear DNA visualization via DAPI staining at the far left, p15 FITC visualization in the middle, while the merged visualizations are at the far right (Original magnification, 20X; scale bar = 50 μm)

SA β-GAL ASSAY OF ZOL-INDUCED SENESCENCE IN OKF 6/TERT-2 AND NHOF CELLS

To further evaluate whether the IC_{50} value could induce senescence, the senescence biomarker, senescence-associated β-galactosidase (SA ß-Gal), was used to measure the degree of senescence in OKF 6/TERT-2 and NHOF cells after ZOL treatment. OKF 6/TERT-2 cells treated with 5-Aza-CdR were served as the positive control. The ZOL-treated OKF 6/TERT-2s (Figure 3(B)) showed evidence of senescence and no significant senescence was detected in the ZOL-treated NHOF (Figure 3(D)). The ZOL-treated OKF 6/TERT-2 cells showed the morphology of enlarged

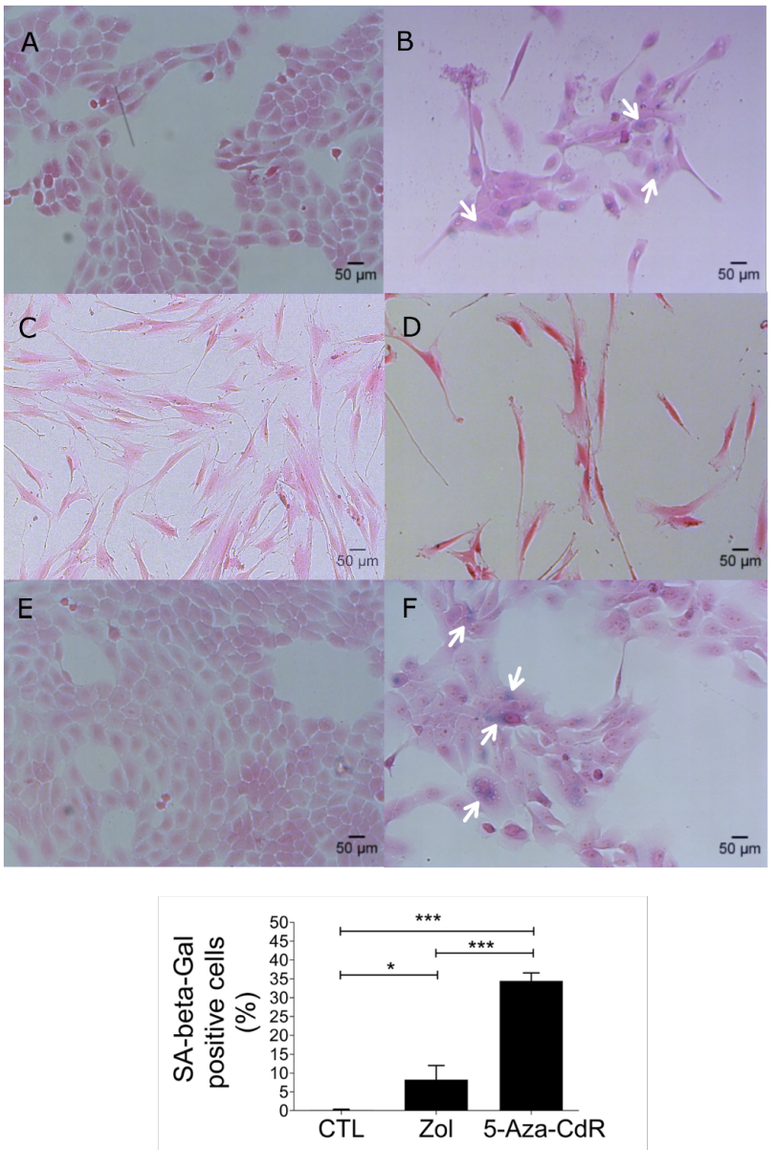

FIGURE 3. Zoledronate induces senescence in immortalized OKF 6/TERT-2 cells. OKF 6/TERT-2 (B) and NHOF(D) cells were treated with 12 µM ZOL for 48 h. Positive SA-β-Gal-stained cells were detected in OKF 6/TERT-2 (B) compared to the control also labeled as CTL (A). However, no blue, SA-β Gal-positive staining was observed in NHOFs (D) compared to the control (C). Positive-stained cells are indicated with white arrows in the photomicrograph. Photomicrographs were taken at 20X. Positive-stained cells were detected (indicated with white arrows in the photomicrograph) in OKF 6/TERT-2 cells tested with 3 µM 5-Aza-CdR for 48 h (F) compared to the control (E). The degree of cell senescence was quantified as the percentage of SA-β-Gal-positive cells after treatment with ZOL as well as 5-Aza-CdR. Asterisk (*) indicates $P \leq 0.05$, and (***) indicates $P \leq 0.001$. Error bars represent the standard error of the mean (SEM) (n=9). (Original magnification: 20X; scale bar=50 µm)

cell size, flattened cell, as well as the appearance of multinucleated and vacuolated cells formed, similar to the appearance of the 5-Aza-CdR-treated positive control (Figure 3(F)). The ZOL-treated OKF 6/TERT-2s contained 8.2 ± 3.8% SA ß-Gal-positive cells, which significantly increased compared to untreated (p = 0.04; n = 9), whereas 5-Aza-CdR-treated OKF 6/TERT-2s contained 34.5 ± 2.1% SA ß-Gal-positive cells (ZOL vs 5-Aza-CdR: $p < 0.0001$; n = 9). Therefore, to further characterize ZOL-induced senescence in 3-dimensional culture, 12 µM was regarded as an appropriate concentration.

HISTOLOGICAL AND IMMUNOHISTOCHEMICAL EXAMINATION OF THE OMM

OKF 6/TERT-2s seeded onto acellular dermis formed multi-layered, regenerated epithelium with the presence of a stratified epithelial layer (Figure 4(A)).

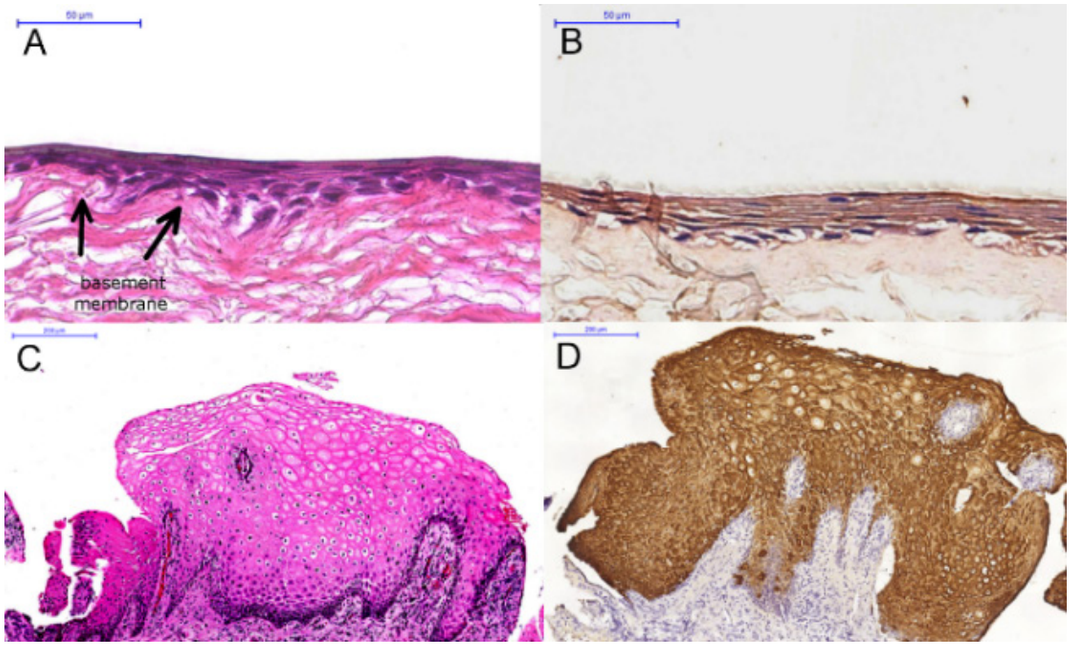

FIGURE 4. Histological analysis of the 3-D oral mucosa model (A, B) in comparison with native mucosa (C, D) using routine hematoxylin & eosin staining (A, C) and detection of CK10/13 via immunohistochemistry (B, D). The undulating surface of the basement membrane of the AlloDerm™ determines the location of attachment of the seeded oral keratinocytes and is indicated by the arrows. (Original magnification, 20X; scale bar = 200 µm and original magnification, 40X; scale bar = 50 µm)

This model consisted of a stratum basale with one layer of columnar to round cells, a relatively flattened stratum spinosum, and a stratum granulosum. Immunohistochemical analyses confirmed the expression of the gingival epithelial markers, cytokeratins 10 and 13 (CK10/13), indicating the preservation of the stratified epithelial barrier (Figure 4(B)). In the untreated model, the epithelial layer remained continuous and was well-stratified (Figure 5(A) & 5(B)).

OMMs treated with ZOL were observed to display discontinuity in the suprabasal layer relative to untreated during the final nine days of treatment. Basal keratinocytes appeared flattened and exhibited a less organized arrangement. Interestingly, treatment with ZOL resulted in a breakage of the BM barrier and epithelial cell migration towards the lamina propria (Figure 5(C) & 5(D)). This histological feature was observed to be relatively consistent with the 5-Aza-CdR-treated model (Figure 5(E) & 5(F)). In the ZOL-treated and 5-Aza-CdR-treated models, 5-6 of these invasions were seen per section. The thinning of the epithelial layer in the ZOL-treated OMM was significant compared to untreated in all three independent experiments. The epithelial thickness of the ZOL-treated tissue was significantly thinner (15.1 ± 4.5 µm) than the untreated model (23.1 ± 7.8 µm) ($P < 0.05$; n = 13) (Figure 5).

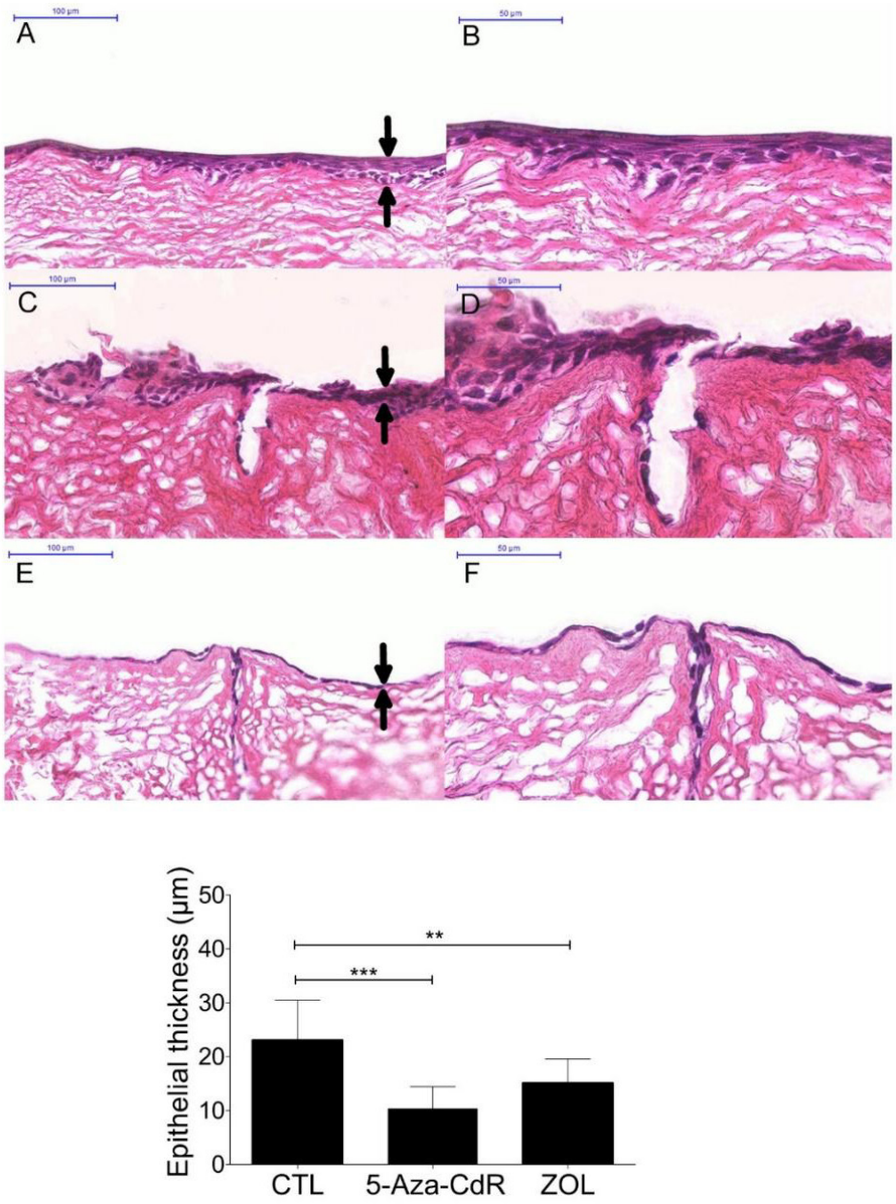

FIGURE 5. The untreated model (labeled as CTL) shows continuously stratified epithelium neither breakage of basement membrane nor downward proliferation of cells (A, B). Histological appearance of ZOL-treated model showing the downward proliferation of epithelial cells toward the lamina propria accompanied by breakage of the basement membrane when treated with ZOL (C, D) Similar histology was observed on the treatment with positive control 5-Aza-CdR (E, F). Arrowhead pointing up indicates the baseline between the basement membrane and lamina propria. Double arrowheads indicate the layer of epithelium stratified on the basement membrane. Figure (A, C, E) is at 20X, and figure (B, D, F) is at 40X magnification. (Original magnification, 20X; scale bar = 100 µm and original magnification, 40X; scale bar = 50 µm). Graph quantitating the epithelial thickness of untreated, ZOL-, and 5-Aza-CdR -treated models. Asterisk (*) indicates P-value ≤ 0.05 and (***) indicates P ≤ 0.001. Error bars represent standard deviation (s.d.) (n = 13)

DETECTION OF SENESCENCE-ASSOCIATED CYTOKINES IN OMM SUPERNATANTS

In the ZOL-treated oral mucosal model, secretion of IL-8 and MMP-3 increased up to 1.5-fold compared to the untreated model (Figure 6(A), 6(B) insets). For the 5-Aza-CdR-treated oral mucosal model, secretion of SASP cytokines increased up to 1.6-fold and 2.8-fold for IL-8 and MMP-3, respectively, compared to the untreated model (Figure 6(A), 6(B) insets).

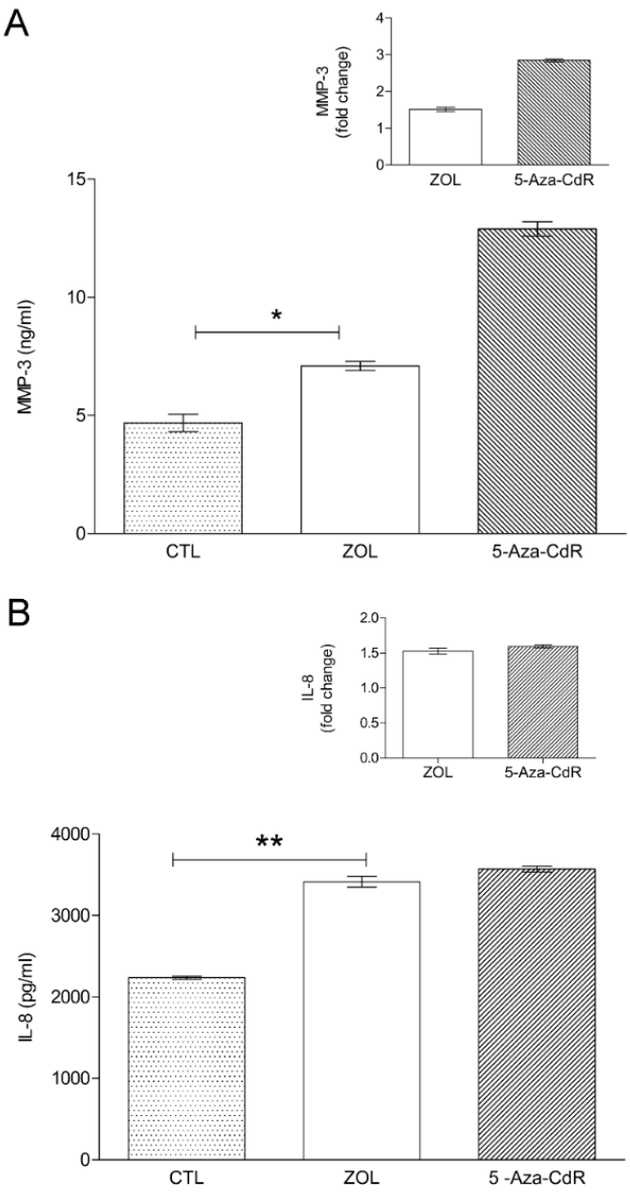

FIGURE 6. MMP-3 (A) and IL-8 (B) were released after exposure of the 3-D oral mucosa model to ZOL as well as 5-Aza-CdR for 48 h. The graph in the inset indicates fold-change values relative to untreated. Asterisk (*) indicates P-value ≤ 0.05 and (**) indicates P ≤ 0.001 vs untreated model. For MMP-3 quantity analysis, untreated model (labelled as CTL) : 4.34 ± 0.52 ng/mL; ZOL-treated oral mucosal model: 7.09 ± 0.27; 5-Aza-CdR-treated oral mucosal model: 12.9 ±0.43 ng/mL. The analysis of quantitative IL-8 expression, untreated model: 2236 ± 25.46 pg/mL; ZOL-treated oral mucosal model: 3415 ±94 pg/mL; 5-Aza-CdR-treated oral mucosal model: 3570 ± 50 pg/mL). Error bars represent standard deviation (s.d.) (n = 3)

DISCUSSION AND CONCLUSION

In agreement with other studies, increased senescence activity was demonstrated in oral keratinocytes treated with N-BPs. Although a previous study suggested that oral keratinocytes underwent senescence and showed decreased proliferation and migration capacity in a wound healing model (Kim et al. 2011), pro-inflammatory phenotypic changes of senescent cells might lead to impaired wound healing in the mucosa had not been entirely investigated. This study chose to investigate the effects of senescence imposed by treatment with ZOL on OMM that contained an intact BM with fibroblasts incorporated as it has been recently shown that SASP molecules secreted by senescent cells can induce changes in tissue histoarchitecture (Freund et al. 2010).

This study's data suggest that cytotoxicity was increased in a time- and dose-dependent manner at a concentration greater than 1 μM, which is consistent with several studies on MRONJ that examined primary normal oral keratinocytes (Ohnuki et al. 2012) and HaCaT cells (Scheper et al. 2009). However, the toxic effect was more significant in OKF 6/TERT-2 cells compared to NHOF. Others have similarly found that fibroblasts have greater viability than oral keratinocytes when tested in monolayer (Ravosa et al. 2011; Ziebart et al. 2011). Therefore, it complicates the choice of ZOL dosage for the oral mucosa model. In the following experiments, 12 μM at 48 h was endorsed as the best concentration after confirming increased senescent positive cells in the SA β-GAL assay.

ZOL inhibited OKF 6/TERT-2 cell growth in a time- and dose-dependent manner; however, there was no appearance of apoptotic bodies. Simultaneous assays to measure apoptosis more definitively would be a future direction. Evidence of apoptosis has been reported in BP treatment by as low as 0.25-3 μM (Scheper et al. 2010) and up to 50 μM (Pabst et al. 2014). In contrast, a study reported no evidence of apoptosis at 10-300 μM when tested with the Alendronate and Risedronate NBPs (Landesberg et al. 2008), and ZOL doses at greater than 100 μM appeared to have a toxic effect that resulted in the detachment of adherent cells and the possibility of necrosis. To the best of the authors' knowledge, no simultaneous apoptosis, necrosis, and senescence inhibitory effects have been reported upon N-BP treatment. Therefore, it is plausible to conclude that in this study, the IC_{50} value of 12 μM increased senescent positive cells compared to the untreated group without exposing cells to the cell death in the forms of apoptosis and necrosis. Valentini et al. (2007) have reported that the IC_{50} dose of VPA (valproic aid) induces cell cycle arrest in M14 melanoma cells by up regulation of $p16^{INK4A}$, p21 and cyclin D1, the common markers of senescence.

There are strong pieces of evidence that support senescence at the onset of MRONJ within oral mucosa. First, it was shown that normal human oral keratinocytes (NHOKs) undergone senescence without accompanying apoptosis, followed by impaired healing and migration in 3D models (Kim et al. 2011). Second, the DNA damage response was also detected in NHOKs, which has been established to share the senescence's activation pathway (Ohnuki et al. 2012). However, a closer examination showed that the NHOKs utilized in this study have a high tendency to eventually enter replicative senescence (Rheinwald et al. 2002).

In the current study, OKF 6/TERT-2 cells were utilized to demonstrate a senescence effect rather than normal human somatic cells in the proposed 3D model. These cells represent normal oral mucosal epithelium immortalized by forced expression of human telomerase (hTERT) via retroviral transduction (Dickson et al. 2000). These cells are less prone to senesce than normal human oral keratinocytes (NHOK) and are therefore more capable of enduring the exhaustive experimental assays of this study. Although immortalized, they retain functional stratification without displaying any cancer-associated changes (Dongari-Bagtzoglou & Kashleva 2006). One of the notable features of both replicative and stress-induced senescence is the participation of the p53-p21 and/or the p15(INK4b) - p16(INK4a) -cyclin D/CDK4-RB1-mediated pathway (RB1 pathway) in the phenotype. Loss of function of one of the cell cycle checkpoints is linked to the promoter hypermethylation, allowing the cell to bypass senescence. Therefore, the capacity of OKF 6/TERT-2s to activate p15 and undergo senescence after treatment with the demethylating agent, 5-Aza-2′-deoxycytidine (referred to as 5-Aza-CdR), was validated. According to the manufacturer, the p15 antibody used in the experiment reacts to the epitope corresponding to amino acids 96-138 of the C-terminus of human p15. On the other hand, treatment with 5-Aza-CdR also activates the senescence program (Lowe et al. 2004) by demethylation of DNA responsible for activating the DNA damage response (Palii et al. 2008) and re-establishing $p15^{INK4b}$ expression (Timmermann et al. 1998). Taken together, p15 has been used as a senescence biomarker in several studies (Collado et al. 2005; Malumbres et al. 2000), which also include 'traditional' SA ß-Gal assays and SAHF (senescence-associated heterochromatin foci) as senescence markers.

This study confirmed that the ZOL treated-OMM showed thinner epithelial layers than the untreated ones after the development of stratified epithelium. This finding is consistent with epithelium thinning described in Ohnuki et al. (2012) when treated with ZOL and another N-BP, pamidronate (Kim et al. 2011). Additionally, this is the first *in vitro* experiment that reports evidence of BM continuity loss and epithelial cell invasion toward the lamina propria upon treatment with ZOL. This histological finding is consistent with ulceration observed mostly in oral alendronate treatment (Kharazmi et al. 2010) and in patients taking zoledronate intravenously (Andreadis et al. 2012), which described ulceration as loss of integrity and a break of tissue deep through the width of the mucosa and basement membrane into the lamina propria (Touyz 2015). This study, therefore, investigated whether the invasion and BM breakage were associated with SASP. Prolonged inflammation has contributed to the release of proteolytic enzymes that favor degradation over tissue repair (Dovi et al. 2004). The SASP factors, MMP-3, and IL-8 were detected in the present model, which is responsible for the malignant phenotypes of epithelial-mesenchyme transition (EMT) and invasiveness (Coppe et al. 2010). These SASP factors have also been used as senescence biomarkers in several studies to detect senescent dermal fibroblasts and melanocytes *in vitro* (Kuilman et al. 2008). Additional senescence markers could be assayed to further confirm the present results.

It is believed that the present findings point toward novel ways to understand how cytotoxic effects of N-BPs, initially serving as bone-targeted therapy, propagate, and induce impaired healing in the oral tissue environment, eventually leading to the exposed bone in the oral cavity. Given that the maintenance of senescence and its paracrine effects are primarily mediated by inflammatory agents, the most likely means of controlling adverse senescence due to bisphosphonate treatment would be anti-inflammatory drugs. Ideally, such drugs would preferentially target senescence-associated inflammatory responses. Further studies will include an investigation measuring a wound-healing protein marker such as cell adhesive protein CCN1, which regulates cell adhesion, migration, and differentiation. Whether anti-inflammatory rescue agents improve the expression profile of CCN1 in the proposed ZOL-treated model is an additional direction with a hope that these findings can inform the improvement of currently available therapies.

ACKNOWLEDGEMENTS

The researchers extend their appreciation to Professor Ian Paterson, who kindly provided the cells required. The authors declare no conflict of interest in this study. This work is supported by the Ministry of Higher Education, Malaysia (UM.C/625/1/HIR/MOHE/DENT/05).

REFERENCES

Andreadis, D., Mauroudis, S., Poulopoulos, A., Markopoulos, A. & Epivatianos, A. 2012. Lip ulceration associated with intravenous administration of zoledronic acid: Report of a case. *Head Neck Pathol.* 6(2): 275-278.

Bae, S., Sun, S., Aghaloo, T., Oh, J.E., McKenna, C.E., Kang, M.K., Shin, K.H. Tetradis, S., Park, N.H. & Kim, R.H. 2014. Development of oral osteomucosal tissue constructs in vitro and localization of fluorescently-labeled bisphosphonates to hard and soft tissue. *Int. J. Mol. Med.* 34(2): 559-563.

Campisi, J. & d'Adda di Fagagna, F. 2007. Cellular senescence: When bad things happen to good cells. *Nat. Rev. Mol. Cell Biol.* 8(9): 729-740.

Collado, M., Gil, J., Efeyan, A., Guerra, C., Schuhmacher, A.J., Barradas, M., Benguria, A., Zaballos, A., Flores, J.M., Barbacid, M., Beach, D. & Serrano, M. 2005. Tumour biology: Senescence in premalignant tumours. *Nature* 436(7051): 642.

Coppe, J.P., Desprez, P.Y., Krtolica, A. & Campisi, J. 2010. The senescence-associated secretory phenotype: The dark side of tumor suppression. *Annu. Rev. Pathol.* 5: 99-118.

Dickson, M.A., Hahn, W.C., Ino, Y., Ronfard, V., Wu, J.Y., Weinberg, R.A., Louis, D.N., Li, F.P. & Rheinwald, J.G. 2000. Human keratinocytes that express hTERT and also bypass a p16(INK4a)-enforced mechanism that limits life span become immortal yet retain normal growth and differentiation characteristics. *Mol. Cell. Biol.* 20(4): 1436-1447.

Dongari-Bagtzoglou, A. & Kashleva, H. 2006. Development of a highly reproducible three-dimensional organotypic model of the oral mucosa. *Nat. Protoc.* 1(4): 2012-2018.

Dovi, J.V., Szpaderska, A.M. & DiPietro, L.A. 2004. Neutrophil function in the healing wound: adding insult to injury? *Thromb Haemost* 92(2): 275-280.

Filleul, O., Crompot, E. & Saussez, S. 2010. Bisphosphonate-induced osteonecrosis of the jaw: A review of 2400 patient cases. *J. Cancer Res. Clin. Oncol.* 136(8): 1117-1124.

Freund, A., Orjalo, A.V., Desprez, P.Y. & Campisi, J. 2010. Inflammatory networks during cellular senescence: Causes and consequences. *Trends Mol. Med.* 16(5): 238-246.

Goodpaster, T., Legesse-Miller, A., Hameed, M.R., Aisner, S.C., Randolph-Habecker, J. & Coller, H.A. 2008. An immunohistochemical method for identifying fibroblasts in formalin-fixed, paraffin-embedded tissue. *J. Histochem. Cytochem.* 56(4): 347-358.

Kharazmi, M., Sjoqvist, K., Rizk, M. & Warfvinge, G. 2010. Oral ulcer associated with alendronate: A case report. *Oral Surg. Oral Med. Oral Pathol. Oral Radiol. Endod.* 110(6): e11-113.

Kim, R.H., Lee, R.S., Williams, D., Bae, S., Woo, J., Lieberman, M., Oh, J.E., Dong, Q., Shin, K.H., Kang, M.K. & Park, N.H. 2011. Bisphosphonates induce senescence in normal human oral keratinocytes. *J. Dent. Res.* 90(6): 810-816.

Kuilman, T., Michaloglou, C., Vredeveld, L.C., Douma, S., Doorn, R.V., Desmet, C.J., Aarden, L.A., Mooi, W.J. & Peeper, D.S. 2008. Oncogene-induced senescence relayed by an interleukin-dependent inflammatory network. *Cell* 133(6): 1019-1031.

Landesberg, R., Cozin, M., Cremers, S., Woo, V., Kousteni, S., Sinha, S., Garrett-Sinha, L. & Raghavan, S. 2008. Inhibition of oral mucosal cell wound healing by bisphosphonates. *J. Oral Maxillofac. Surg.* 66(5): 839-847.

Lowe, S.W., Cepero, E. & Evan, G. 2004. Intrinsic tumour suppression. *Nature* 432(7015): 307-315.

Malumbres, M., Castro, I.P.D., Hernandez, M.I., Jimenez, M., Corral, T. & Pellicer, A. 2000. Cellular response to oncogenic Ras involves induction of the Cdk4 and Cdk6 inhibitor p15(INK4b). *Mol. Cell Biol.* 20(8): 2915-2925.

Nicolatou-Galitis, O., Schiodt, M., Mendes, R.A., Ripamonti, C., Hope, S., Drudge-Coates, L., Niepel, D. & den Wyngaert, T.V. 2019. Medication-related osteonecrosis of the jaw: Definition and best practice for prevention, diagnosis, and treatment. *Oral Surg. Oral Med. Oral Pathol. Oral Radiol.* 127(2): 117-135.

Ohnuki, H., Izumi, K., Terada, M., Saito, T., Kato, H., Suzuki, A., Kawano, Y., Nozawa-Inoue, K., Takagi, R. & Maeda, T. 2012. Zoledronic acid induces S-phase arrest via a DNA damage response in normal human oral keratinocytes. *Arch Oral Biol.* 57(7): 906-917.

Pabst, A.M., Ziebart, T., Ackermann, M., Konerding, M.A. & Walter, C. 2014. Bisphosphonates' antiangiogenic potency in the development of bisphosphonate-associated osteonecrosis of the jaws: influence on microvessel sprouting in an *in vivo* 3D Matrigel assay. *Clin. Oral Investig*. 18(3): 1015-1022.

Palii, S.S., Emburgh, B.O.V., Sankpal, U.T., Brown, K.D. & Robertson, K.D. 2008. DNA methylation inhibitor 5-Aza-2'-deoxycytidine induces reversible genome-wide DNA damage that is distinctly influenced by DNA methyltransferases 1 and 3B. *Mol. Cell Biol.* 28(2): 752-771.

Ravosa, M.J., Ning, J., Liu, Y. & Stack, M.S. 2011. Bisphosphonate effects on the behaviour of oral epithelial cells and oral fibroblasts. *Archives of Oral Biology* 56(5): 491-498.

Reid, I.R. 2009. Osteonecrosis of the jaw: Who gets it, and why? *Bone* 44(1): 4-10.

Rheinwald, J.G., Hahn, W.C., Ramsey, M.R., Wu, J.Y., Guo, Z., Tsao, H., Luca, M.D., Catricala, C. & O'Toole, K.M. 2002. A two-stage, p16(INK4A)- and p53-dependent keratinocyte senescence mechanism that limits replicative potential independent of telomere status. *Mol. Cell Biol.* 22(14): 5157-5172.

Scheper, M., Chaisuparat, R., Cullen, K. & Meiller, T. 2010. A novel soft-tissue *in vitro* model for bisphosphonate-associated osteonecrosis. *Fibrogenesis Tissue Repair* 3: 6-17.

Scheper, M.A., Badros, A., Chaisuparat, R., Cullen, K.J. & Meiller, T.F. 2009. Effect of zoledronic acid on oral fibroblasts and epithelial cells: A potential mechanism of bisphosphonate-associated osteonecrosis. *Br. J. Haematol.* 144(5): 667-676.

Timmermann, S., Hinds, P.W. & Munger, K. 1998. Re-expression of endogenous p16ink4a in oral squamous cell carcinoma lines by 5-aza-2'-deoxycytidine treatment induces a senescence-like state. *Oncogene* 17(26): 3445-3453.

Touyz, L.Z.G. 2015. Bisphosphonate osteo-necrosis of the jaws [BONJ], from defective function of oral epithelial intercellular junctions? *Medical Hypotheses* 84: 474-476.

Tra, W.M.W., van Neck, J.W., Hovius, S.E.R., van Osch, G.J.V.M. & Perez-Amodio, S. 2012. Characterization of a three-dimensional mucosal equivalent: Similarities and differences with native oral mucosa. *Cells Tissues Organs* 195(3): 185-196.

Valentini, A., Gravina, P., Federici, G. & Bernardini, S. 2007. Valproic acid induces apoptosis, p16INK4A upregulation and sensitization to chemotherapy in human melanoma cells. *Cancer Biol. Ther.* 6(2): 185-191.

Yuan, D., Ye, S., Pan, Y., Bao, Y., Chen, H. & Shao, C. 2013. Long-term cadmium exposure leads to the enhancement of lymphocyte proliferation via down-regulating p16 by DNA hypermethylation. *Mutat. Res.* 757(2): 125-131.

Ziebart, T., Koch, F., Klein, M.O., Guth, J., Adler, J., Pabst, A., Al-Nawas, B. & Walter, C. 2011. Geranylgeraniol - A new potential therapeutic approach to bisphosphonate associated osteonecrosis of the jaw. *Oral Oncol.* 47(3): 195-201.

*Corresponding author; email: chaiwl@um.edu.my